LETTERS

Crystal structure of the neurotrophin-3 and p75^{NTR} symmetrical complex

Yong Gong[1]*, Peng Cao[1]*, Hong-jun Yu[1] & Tao Jiang[1]

Neurotrophins (NTs) are important regulators for the survival, differentiation and maintenance of different peripheral and central neurons. NTs bind to two distinct classes of glycosylated receptor: the p75 neurotrophin receptor (p75^{NTR}) and tyrosine kinase receptors (Trks). Whereas p75^{NTR} binds to all NTs, the Trk subtypes are specific for each NT[1,2]. The question of whether NTs stimulate p75^{NTR} by inducing receptor homodimerization is still under debate. Here we report the 2.6-Å resolution crystal structure of neurotrophin-3 (NT-3) complexed to the ectodomain of glycosylated p75^{NTR}. In contrast to the previously reported asymmetric complex structure, which contains a dimer of nerve growth factor (NGF) bound to a single ectodomain of deglycosylated p75^{NTR} (ref. 3), we show that NT-3 forms a central homodimer around which two glycosylated p75^{NTR} molecules bind symmetrically. Symmetrical binding occurs along the NT-3 interfaces, resulting in a 2:2 ligand–receptor cluster. A comparison of the symmetrical and asymmetric structures reveals significant differences in ligand–receptor interactions and p75^{NTR} conformations. Biochemical experiments indicate that both NT-3 and NGF bind to p75^{NTR} with 2:2 stoichiometry in solution, whereas the 2:1 complexes are the result of artificial deglycosylation. We therefore propose that the symmetrical 2:2 complex reflects a native state of p75^{NTR} activation at the cell surface. These results provide a model for NTs-p75^{NTR} recognition and signal generation, as well as insights into coordination between p75^{NTR} and Trks.

NGF, brain-derived neurotrophic factor (BDNF) and NT-3 are members of neurotrophin family, which engage two types of single-transmembrane cell-surface receptor Trks and p75^{NTR} to perform a wide variety of functions in the mammalian nervous system. TrkA, TrkB and TrkC are the cognate receptors of NGF, BDNF and NT-3, respectively, and NT-3 also binds to TrkA and TrkB with low affinity[1,2]. p75^{NTR} is a 75-kDa glycoprotein, which can bind all NTs and proneutrophins (proNTs). p75^{NTR} belongs to the tumour necrosis factor receptor (TNFR) superfamily, which is structurally characterized by having extracellular cysteine-rich domains (CRDs) and an intracellular death domain. Signalling pathways mediated by p75^{NTR} promote either cell survival or, paradoxically, cell apoptosis. p75^{NTR} can function as a positive modulator of Trks by creating high-affinity binding sites for NTs[4]. However, the binding mode between NTs and p75^{NTR} and the crosstalk mechanism between Trk and p75^{NTR} have remained unknown. Whereas one crystallography study indicated a 2:1 asymmetric binding complex formed between NGF and the ectodomain of deglycosylated p75^{NTR} (dg-p75^{NTR})[3], another biochemical report indicated that a symmetrical 2:2 stoichiometric binding complex formed between NGF and glycosylated p75^{NTR} (ref. 5). To elucidate the interaction mechanism between p75^{NTR} and NTs, we crystallized the ectodomain of glycosylated p75^{NTR} in complex with NT-3.

Crystal complexes were prepared from recombinant human NT-3 and the ectodomain of rat glycosylated p75^{NTR} (size-exclusion chromatography is shown in Supplementary Fig. 1), and the crystal structure has been determined to 2.6 Å resolution. In contrast with previous reports, we found that the NT-3–p75^{NTR} complex contains a central NT-3 homodimer with two symmetrically arranged p75^{NTR} molecules in the clefts between the NT-3 subunits (Fig. 1). The complex has a perfect non-crystallographic two-fold symmetry axis, which we suggest lies perpendicular to the cell membrane, and the root mean square deviation (r.m.s.d.) value between the two sides of the dimer is about 0.30 Å. Each p75^{NTR} protomer is about 110 Å long, and the amino and carboxy termini protrude beyond both the top and bottom ends of the NT-3 dimer. The two p75^{NTR} protomers have parallel conformations, with four kinked CRDs (CRD1–CRD4) arranged in tandem. Twelve pairs of disulphide bonds are evenly spaced along p75^{NTR}. CRD1, which includes Asn 32, is located distal to the cell membrane. CRD2, CRD3 and CRD4 interact the most with NT-3. The two p75^{NTR} C termini extend towards each other with a minor interface of about 95 Å^2.

A total solvent-accessible surface of about 2,314 Å^2 is buried between the NT-3 dimer and each copy of p75^{NTR}. A detailed analysis of the ligand–receptor contacts is shown in Fig. 2 and Supplementary Table 1. The interface can be divided into three main contact sites on p75^{NTR} that are stabilized by hydrophobic interactions, salt bridges and hydrogen bonds. The junction regions between CDR1 and CDR2, with CRD2 taking the predominant role, create site 1. Site 1 is an extensively hydrogen-bonded network, containing five hydrogen bonds and one salt bridge (Fig. 2a). Site 2 is formed by equal contributions from CDR3 and CRD4 and involves two salt bridges and two hydrogen bonds (Fig. 2b). Site 3 includes only one salt bridge between Lys 73A of NT-3 and Glu 143 of the p75^{NTR} C-terminal loop

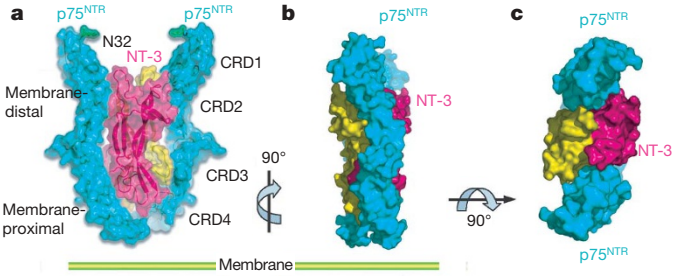

Figure 1 | Architecture of the NT-3–p75^{NTR} complex. a, Ribbon and surface diagram of the complex. One NT-3 monomer is shown in red and the other in yellow, and p75^{NTR} is shown in blue. The N-linked carbohydrates at Asn 32 of p75^{NTR} are shown in green. **b**, Surface representation equivalent of **a**, rotated by 90° around the vertical. **c**, As in **b**, but rotated by 90° around the horizontal.

[1]National Key Laboratory of Biomacromolecules, Institute of Biophysics, Chinese Academy of Sciences, 15 Datun Road, Chaoyang District, Beijing 100101, China.
*These authors contributed equally to this work.

(Fig. 2c). Sequence alignments (Fig. 2d) show that the p75^{NTR} contact residues are, for the most part, conserved across all NTs.

In contrast to other members of the TNFR superfamily, such as TNFβ–TNFR[6] and TRAIL–DR5 (ref. 7), which are activated as preformed trimeric receptor complexes by trimeric ligands, p75^{NTR} is induced to form a dimer by dimeric NT-3 ligand. However, they share a common binding style in which the receptors bind along the seam of the interfaces between two ligands to form symmetrical complexes.

A detailed comparison with the structure of the unbound homodimer NT-3 (ref. 8) shows that conformational changes are induced by the binding of p75^{NTR} (Fig. 3a). First, the surface area buried at the interface of the two NT-3 monomers in the complex structure is about 2,960 Å^2, which is slightly smaller than the 3,190 Å^2 surface area in the unbound state. It results in an r.m.s.d. of 1.21 Å of the whole dimer to avoid short contacts with the receptors. Second, a prominent conformational change occurs at residues 5–12 in the N-terminal loop, which was shown to have a key function in receptor binding[9]. In the bound state, the tail of NT-3 sways to form a critical part of the interface with p75^{NTR} through hydrogen bonds and hydrophobic interactions. The other conformational differences are situated mainly at the interface with p75^{NTR}, such as movements in loops 40–48 and 70–76 and the residues Arg 31, Glu 59, Asn 65, Leu 96 and Arg 114.

Trks are known to dimerize by means of a 2:2 NT-induced clustering activation mechanism that triggers the signal transduction cascade[10,11]. The molecular arrangements of TrkA and p75^{NTR} on NTs have opposite orientations. Although both receptors bind to the seam of the NT dimer, TrkA interacts with the middle concave face, whereas p75^{NTR} binds separately to the two convex faces (Fig. 3b–d). The buried face between the NT-3 dimer and p75^{NTR} (2,314 Å^2) is very similar to that between NGF and TrkA (2,245 Å^2), in line with the observation that both receptors bind all NTs with an equilibrium binding constant when expressed alone[1]. The N-terminal tails of the NTs adopt quite different conformations and directions in both structures, permitting specificity of NT interaction for different receptors.

Comparison of our structure with a previous asymmetric NGF–p75^{NTR} complex[3] reveals differences. First, NGF is a distorted dimer in the asymmetric complex, which leads to the hypothesis that p75^{NTR} binding to one side of NGF induces a bending of the entire NGF and disabling binding of a second p75^{NTR} to the opposite site. In contrast, NT-3 is a perfect homodimer in our structure, and the p75^{NTR} receptors bind symmetrically to form a 2:2 cluster. Second, we observed significant differences in conformation between the p75^{NTR} molecules in two structures (Fig. 4a). The most prominent conformational change concerns the N-terminal CRD1 and CRD2 of

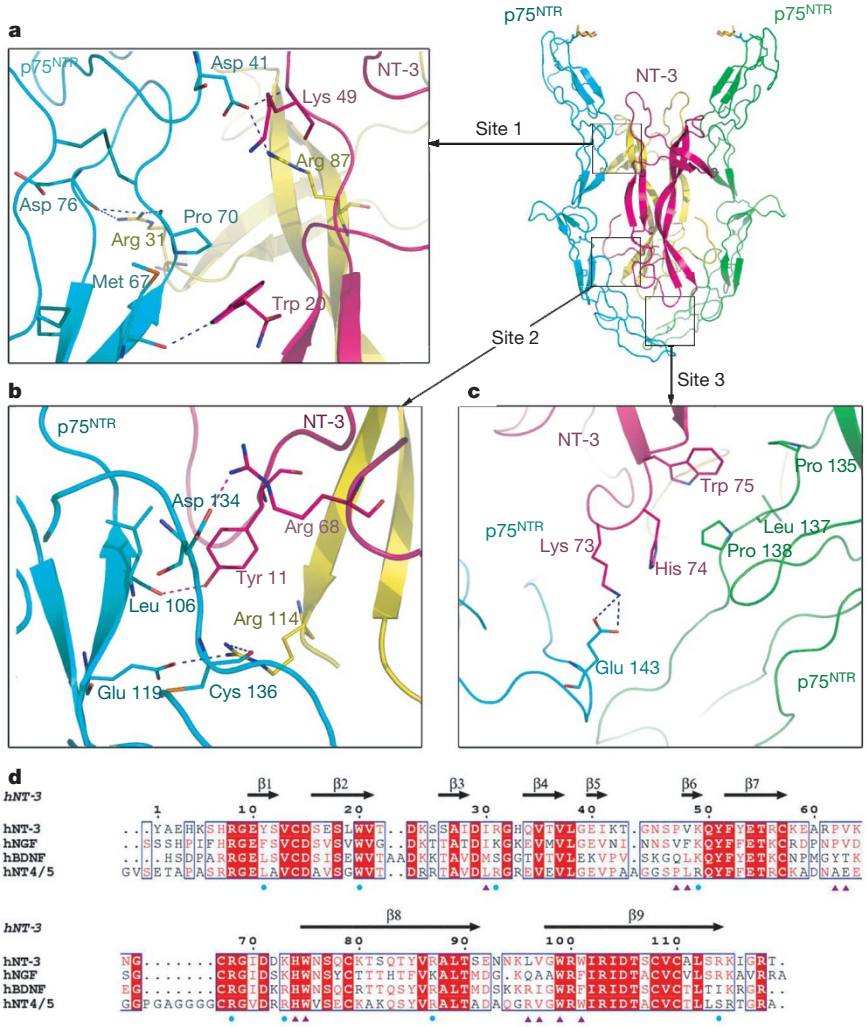

Figure 2 | Interactions between p75^{NTR} and NT-3. **a**, Close-up of the site 1 interface. NT-3 monomers are shown in red and yellow, and p75^{NTR} is shown in blue and green. Hydrogen bonds and salt bridges are shown as dashed lines. **b**, **c**, Close-ups of the site 2 (**b**) and site 3 (**c**) interfaces. **d**, Human (h) neurotrophin family sequence alignments for NT-3, NGF, BDNF and NT4/5. Strictly conserved and conservatively substituted residues are boxed and indicated by a red background or red letters, respectively. Hydrogen bonds and salt bridges with p75^{NTR} are marked below the alignments by blue dots, and hydrophobic contacts are indicated by purple triangles.

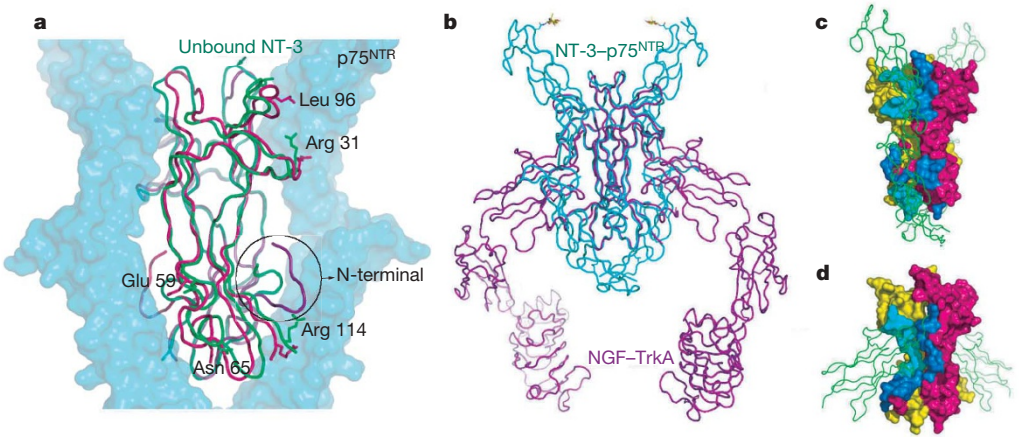

Figure 3 | Structural comparison. **a**, Comparison of bound and unbound human NT-3. Unbound human NT-3 is shown in green, bound NT-3 in red and purple, and p75^{NTR} in blue. The N terminus is circled, and the labelled amino acids show notably different conformations. **b**, Comparison of the NT-3–p75^{NTR} complex (blue) with the NGF–TrkA ectodomain complex (purple). **c**, **d**, The regions at the surfaces of NT-3 (**c**) and NGF (**d**) that are buried by p75^{NTR} and TrkA, respectively. NT monomers are shown in red and yellow, and p75^{NTR} or TrkA is shown in green. The light and deep blue areas indicate the binding surfaces on each monomer.

p75^{NTR} with an r.m.s.d. of about 3.5 Å (Fig. 4b), resulting in changes in the interacting pairs of residues that bind NTs. Despite a better agreement in CRD3 and CRD4 (r.m.s.d. about 0.7 Å; Fig. 4c), there are also structural differences in the C-terminal loops (residues 140–152). Third, our structure is tethered together through three separate binding sites on p75^{NTR}, whereas the asymmetric complex is tethered through only two sites (sites 1 and 2). At site 1, our structure has two more hydrogen bonds and one less salt bridge than the asymmetric structure. Site 2 has an additional hydrogen bond compared with the asymmetric structure between Leu 106 of p75^{NTR} and Tyr 11B of NT-3. This hydrogen bond is determined by NT-3 because the corresponding residues to Tyr 11 are Phe 12, Leu 10 and Leu 14 on NGF, BDNF and NT4/5, respectively. The largest difference in two structures is at site 3. The C-terminal loop of p75^{NTR} in our structure sways close to NT-3, allowing the formation of a salt bridge with the 'Lys 73-His-Trp 75' loop in NT-3, which is conserved in NTs. No interaction closer than 6 Å was observed at this binding site in the asymmetric structure.

Previous studies indicated that p75^{NTR} binds to NGF and NT-3 with similar affinities[12]; however, it was still unclear whether differences between NGF and NT-3 could alter the binding stoichiometry. We measured the ligand–receptor stoichiometry of p75^{NTR} in a complex with NGF or NT-3 in solution by analytical ultracentrifugation. The results indicate that both NGF and NT-3 bind to p75^{NTR} with a 2:2 stoichiometry (Fig. 4d and Supplementary Fig. 2). These results are consistent with a report[5] showing a 2:2 stoichiometry of human p75^{NTR} and NGF with the use of mass spectrometry, analytical ultracentrifugation and solution X-ray scattering measurements.

Glycans have a pivotal function in protein folding, oligomerization, sorting and transport in the endoplasmic reticulum and in the early secretory pathway[13]. In addition, the importance of p75^{NTR} N-linked glycosylation in NGF signalling has been demonstrated in PC12 cells[14]. We therefore investigated the influence of glycosylation on p75^{NTR} by expressing dg-p75^{NTR} and using Biacore analysis to measure its association constant with NT-3. We found that dg-p75^{NTR} had a significantly lower affinity than p75^{NTR} for NT-3

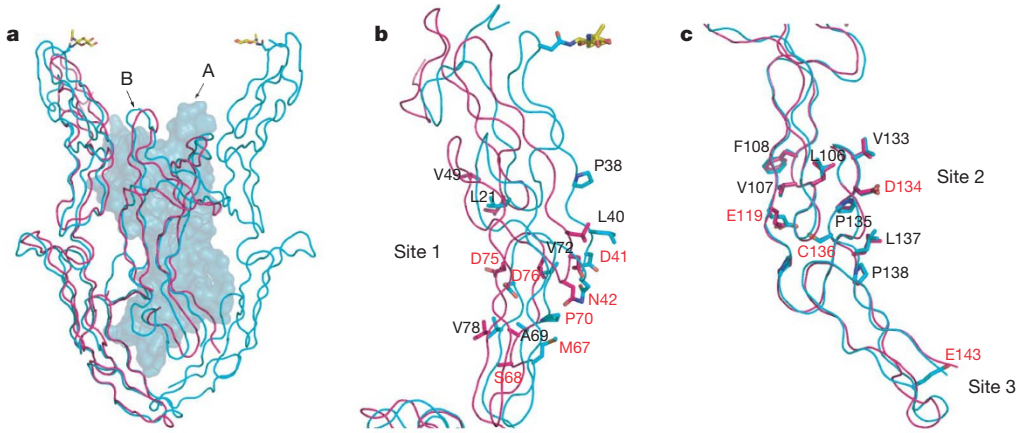

d

Molecular mass	p75^{NTR}	hNT-3–p75^{NTR}	hNGF–p75^{NTR}	mNGF–p75^{NTR}	dg–p75^{NTR}	hNT-3–dg-p75^{NTR}	hNGF–dg-p75^{NTR}
Measured (kDa)	21.3	67.8	68.4	71.0	19.2	45.5	45.1
Theoretical (kDa)	20.1	66.2 (2:2)	66.4 (2:2)	66.2 (2:2)	18.7	44.8 (2:1)	44.9 (2:1)

Figure 4 | Comparison of the 2:2 NT-3–p75^{NTR} complex with the 2:1 NGF–dg-p75^{NTR} complex. **a**, An overall view of the 2:2 complex (blue) and the 2:1 complex (red). Monomer A of NT-3 is shown as a molecular surface. **b**, **c**, A detailed comparison of the p75^{NTR} conformation and interactions with NT-3 or NGF. **b**, The N-terminal half of p75^{NTR}. **c**, The C-terminal half of p75^{NTR}. The residues involved with hydrophobic interactions and hydrogen bonds (or salt bridges) are labelled in black and red, respectively. **d**, Analytical ultracentrifugation analysis of p75^{NTR}, dg-p75^{NTR} and complexes with NTs; h, human; m, mouse. The measured and theoretical molecular masses are indicated.

(Supplementary Fig. 3). Using analytical ultracentrifugation, we detected unliganded dg-p75^{NTR} as a mixture of monomers and dimmers (Supplementary Fig. 4), in contrast to unliganded p75^{NTR}, which we detected as strictly monomers (Supplementary Fig. 2). These data suggest that dg-p75^{NTR} has different properties from those of native p75^{NTR}.

The stoichiometries of dg-p75^{NTR} in complex with NT-3 or NGF were further examined by analytical ultracentrifugation. For both NT-3–dg-p75^{NTR} and NGF–dg-p75^{NTR} we observed only the 2:1 complexes (Fig. 4d and Supplementary Fig. 4). These results are consistent with a previous report[3] and indicate that formation of the 2:1 complex is related to receptor deglycosylation. We therefore conclude that the 2:2 ligand–receptor stoichiometry is the native and common mode of both NT-3 and NGF binding to glycosylated p75^{NTR}, whereas the 2:1 complexes are the result of artificial deglycosylation.

In our structure, only the first sugar (GlcNAc) of the five to eight carbohydrates in the N-glycan of Asn 32 was well defined by the electron density map. Although GlcNAc was not observed to make direct contacts with NT-3, the entire sugar chain probably has a function in the structural conformation and stabilization of p75^{NTR}, and in turn can affect its ligand binding activity. Similar cases were also reported for the structures of TrkA complexed with NGF[11] and the natriuretic peptide receptor with C-type natriuretic peptide[15], in which the carbohydrate moieties on the receptors do not contact the ligands but modulate the ligand-binding activities of receptors.

The 2:2 architecture of the complex establishes a NT-induced dimerization model for p75^{NTR} activation. Two receptors bind along the interface surface grooves symmetrically, resulting in a 2:2 ligand–receptor cluster. The role of NT-3 in receptor dimerization seems to be critical, because there is little protein–protein contact between two p75^{NTR} receptors in our structure but significant contacts occur between NT-3 and p75^{NTR}, which facilitates the homodimerization of p75^{NTR}. The 2:2 cluster may result in bringing the C termini of two receptors into such close contact that the cytoplasmic regions, particularly the death domains, come into contact. This process facilitates the recruitment of intracellular interactors to generate signals downstream. Receptor clustering has been recognized as a general signal transduction mechanism for growth-factor receptors[16]. The high structural conservation of NTs (Fig. 2d) and biochemical results lead us to propose that the 2:2 symmetrical complex reflects the native activated state of p75^{NTR} at the cell surface when bound to NTs, providing a ubiquitous model for p75^{NTR} recognition, activation and signal generation.

The crosstalk between p75^{NTR} and Trks creates high-affinity NT-binding sites on neuronal cells and alters the signalling properties of both partners through poorly understood mechanisms[17]. However, the superposition of our structure on the crystal structure of the ectodomain of TrkA and NGF complex[10,11,18] shows that there are mutually exclusive binding sites on the ligands. It is therefore impossible for a p75^{NTR}–NT–TrkA ternary complex to form a high-affinity binding site or an instantaneous intermediate binding state through interactions between extracellular domains of the receptors. Instead, the ectodomains of NT receptors simply share a ligand-competing relationship, rather than direct interactions. The high-affinity binding site probably occurs through the cytosolic and transmembrane domains of p75^{NTR} and Trks. These interactions may be not direct but facilitated by the pool of intracellular interaction partners and transmembrane constituents, which form a bridge between p75^{NTR} and Trks.

Although the precise mechanism of how limited combinations of distinct NTs and their receptors can produce such a multitude of specific cell responses is still unknown, we propose that the current 2:2 symmetrical NT-3–p75^{NTR} complex represents a native active state for NT-3–p75^{NTR} interaction during neuronal development. This symmetrical NT-3–p75^{NTR} complex provides a molecular basis for the recognition of receptors for NTs and signal transduction mechanisms. Our structure also provides critical insights, which may allow the design of specific NTs agonists for the fine tuning of neuronal development.

METHODS SUMMARY

Protein expression. The rat p75^{NTR} ectodomain, which shares 94% identity with human p75^{NTR}, was expressed in sf9 cells. The secreted soluble p75^{NTR} protein was N-glycosylated at residue Asn 32 of the mature protein. The protein was purified by affinity chromatography and gel filtration. Recombinant human NT-3 and human NGF were expressed in *Escherichia coli* (Genentech). To form the complex, p75^{NTR} (20 mg ml^{-1}) and NT-3 (20 mg ml^{-1}) were mixed at a concentration ratio of 1.5:1. Deglycosylated p75^{NTR} was produced by using tunicamycin to inhibit glycosylation.

Crystallography. Crystals of the NT-3–p75^{NTR} complex were grown by hanging-drop vapour diffusion at 17 °C. X-ray diffraction data were collected at EMBL beamline BW7A (Hamburg) to a resolution of 2.6 Å, and were integrated and scaled with DENZO and SCALEPACK[19]. The structure was determined by molecular replacement with two models of human NT-3 (PDB code 1NT3) and the partial C-terminal half of p75^{NTR} from the NGF–p75^{NTR} 2:1 asymmetric complex (PDB code: 1SG1) using the program Molrep[20] from the CCP4 program suite[21]. The remaining structure was traced by Coot[22] independently into the electron density map, which was calculated with partial phases. The structure was refined with Refmac[23] to an R_{work}/R_{free} of 22.4%/28.8%. All images were prepared with Pymol[24] except Fig. 2d, which was generated with ESPript[25]. Crystallographic data are provided in Supplementary Table 2.

Full Methods and any associated references are available in the online version of the paper at www.nature.com/nature.

Received 10 April; accepted 16 May 2008.
Published online 2 July 2008.

1. Schweigreiter, R. The dual nature of neurotrophins. *BioEssays* **28,** 583–594 (2006).
2. Bothwell, M. Functional interactions of neurotrophins and neurotrophin receptors. *Annu. Rev. Neurosci.* **18,** 223–253 (1995).
3. He, X. L. & Garcia, K. C. Structure of nerve growth factor complexed with the shared neurotrophin receptor p75. *Science* **304,** 870–875 (2004).
4. Nykjaer, A., Willnow, T. E. & Petersen, C. M. p75^{NTR}—live or let die. *Curr. Opin. Neurobiol.* **15,** 49–57 (2005).
5. Aurikko, J. P. *et al.* Characterization of symmetric complexes of nerve growth factor and the ectodomain of the pan-neurotrophin receptor, p75^{NTR}. *J. Biol. Chem.* **280,** 33453–33460 (2005).
6. Banner, D. W. *et al.* Crystal structure of the soluble human 55 kd TNF receptor–human TNFβ complex: implications for TNF receptor activation. *Cell* **73,** 431–445 (1993).
7. Mongkolsapaya, J. *et al.* Structure of the TRAIL–DR5 complex reveals mechanisms conferring specificity in apoptotic initiation. *Nature Struct. Biol.* **6,** 1048–1053 (1999).
8. Butte, M. J., Hwang, P. K., Mobley, W. C. & Fletterick, R. J. Crystal structure of neurotrophin-3 homodimer shows distinct regions are used to bind its receptors. *Biochemistry* **37,** 16846–16852 (1998).
9. McInnes, C. & Sykes, B. D. Growth factor receptors: structure, mechanism, and drug discovery. *Biopolymers* **43,** 339–366 (1997).
10. Wiesmann, C., Ultsch, M. H., Bass, S. H. & de Vos, A. M. Crystal structure of nerve growth factor in complex with the ligand-binding domain of the TrkA receptor. *Nature* **401,** 184–188 (1999).
11. Wehrman, T. *et al.* Structural and mechanistic insights into nerve growth factor interactions with the TrkA and p75 receptors. *Neuron* **53,** 25–38 (2007).
12. Rodriguez-Tebar, A., Dechant, G., Gotz, R. & Barde, Y. A. Binding of neurotrophin-3 to its neuronal receptors and interactions with nerve growth factor and brain-derived neurotrophic factor. *EMBO J.* **11,** 917–922 (1992).
13. Helenius, A. & Aebi, M. Intracellular functions of N-linked glycans. *Science* **291,** 2364–2369 (2001).
14. Baribault, T. J. & Neet, K. E. Effects of tunicamycin on NGF binding and neurite outgrowth in PC12 cells. *J. Neurosci. Res.* **14,** 49–60 (1985).
15. He, X., Chow, D., Martick, M. M. & Garcia, K. C. Allosteric activation of a spring-loaded natriuretic peptide receptor dimer by hormone. *Science* **293,** 1657–1662 (2001).
16. Ullrich, A. & Schlessinger, J. Signal transduction by receptors with tyrosine kinase activity. *Cell* **61,** 203–212 (1990).
17. Reichardt, L. F. Neurotrophin-regulated signalling pathways. *Phil. Trans. R. Soc. B* **361,** 1545–1564 (2006).
18. Barker, P. A. High affinity not in the vicinity? *Neuron* **53,** 1–4 (2007).
19. Otwinowski, Z. & Minor, W. Processing of X-ray diffraction data collected in oscillation mode. *Methods Enzymol.* **276,** 307–326 (1997).
20. Vagin, A. & Teplyakov, A. MOLREP: an automated program for molecular replacement. *J. Appl. Cryst.* **30,** 1022–1025 (1997).
21. Project, C. C. The CCP4 suite: programs for protein crystallography. *Acta Crystallogr. D Biol. Crystallogr.* **50,** 760–763 (1994).

22. Emsley, P. & Cowtan, K. Coot: model-building tools for molecular graphics. *Acta Crystallogr. D Biol. Crystallogr.* **60,** 2126–2132 (2004).
23. Murshudov, G. N., Vagin, A. A. & Dodson, E. J. Refinement of macromolecular structures by the maximum-likelihood method. *Acta Crystallogr. D Biol. Crystallogr.* **53,** 240–255 (1997).
24. Delano, W. L. The PyMOL Molecular Graphics System, DeLano Scientific, San Carlos, CA, USA (2002).
25. Gouet, P., Courcelle, E., Stuart, D. I. & Metoz, F. ESPript: analysis of multiple sequence alignments in PostScript. *Bioinformatics* **15,** 305–308 (1999).

Supplementary Information is linked to the online version of the paper at www.nature.com/nature.

Acknowledgements We thank X. X. Yu for help with analytical ultracentrifugation assay, and Y. Y. Chen for the BIAcore assay. We thank Genentech for the gift of recombinant human NT-3 and recombinant human NGF. This research was supported financially by the National Key Basic Research Program, the National Natural Science Foundation of China and the National High Technology Research and Development Program of China.

Author Contributions T.J. supervised the project. Y.G. expressed, purified and crystallized the complex and performed biochemical assays. P.C. determined the structure of the complex. H.J.Y. helped with its expression and purification. P.C., Y.G. and T.J. interpreted data and wrote the paper.

Author Information Atomic coordinates and structure factors have been deposited in the Protein Data Bank under accession code 3BUK. Reprints and permissions information is available at www.nature.com/reprints. Correspondence and requests for materials should be addressed to T.J. (tjiang@ibp.ac.cn).

METHODS

Cloning and plasmid construction. A construct encoding the extracellular domain (residues 1–161) of $p75^{NTR}$ was amplified from the rat $p75^{NTR}$ cDNA by polymerase chain reaction and cloned into pFastbac1, which was modified by adding an N-terminal honeybee melittin signal peptide and a C-terminal hexahistidine tag. Recombinant baculovirus was produced and amplified with *Spodoptera frugiperda* (Sf9) cells in serum-containing *Trichoplusia ni* medium–Fred Hink (TNM-FH) insect medium at 27 °C.

Expression and purification of proteins. The Sf9 cells were cultivated in flasks in 2.5 l of serum-free HyQ SFX medium (HyClone) at 27 °C. When the cell density reached 5×10^6 cells per millilitre, the cells were centrifuged and resuspended in 2.5 l of fresh serum-free medium and were infected with recombinant virus at a multiplicity of infection of more than 5. The supernatant of the cultures was collected 72 h after infection. The expressed protein was purified by metal-affinity chromatography on chelatin resin and size-exclusion chromatography on a Superdex 200 10/300 GL column (GE, shown in Supplementary Fig. 1). Deglycosylated $p75^{NTR}$ was produced with tunicamycin to inhibit glycosylation. Recombinant human neurotrophin-3 (hNT-3) and human nerve growth factor (hNGF) were expressed from *Escherichia coli* (a gift from Genentech). Murine NGF was obtained from the submaxillary glands of mice (AbD Serotec).

Crystallization, data collection and structure determination. For crystallization, the purified $p75^{NTR}$ and NT-3 proteins were each concentrated and buffer-exchanged with 10 mM Tris-HCl (pH 7.5) buffer at a concentration of about 20 mg ml^{-1}. Crystals of the NT-3–$p75^{NTR}$ complex were grown at 17 °C by hanging-drop vapour diffusion from a mixture of $p75^{NTR}$ and NT-3 at a concentration ratio of 1.5:1. Initially, crystallization was performed under the conditions provided by the commercially available crystallization screening kits Screen I and II (Hampton Research); microcrystals were obtained in this way. After the reservoir solutions had been optimized, better crystals were obtained by mixing 1 μl of protein solution with 1 μl of reservoir solution and equilibrating against 1 ml of reservoir solution containing 0.9 M lithium sulphate, 0.05 M sodium citrate (pH 5.0) and 0.7 M ammonium sulphate. Block-like crystals appeared after incubation for 3–5 days and matured to their full sizes (typically, 0.3 mm × 0.2 mm × 0.2 mm) within 2 weeks.

Before data collection, the crystal was cryoprotected by being soaked briefly in paratone oil (Hampton Research) and flash-cooled in liquid nitrogen. X-ray diffraction data were collected to 2.6 Å by using EMBL beamline BW7A at 100 K and at a wavelength of 1.0030 Å. The data were integrated and scaled with DENZO and SCALEPACK software. The crystal has space group $R3$ with unit-cell dimensions of $a = b = 125.8$ Å and $c = 133.1$ Å.

Crystal structure was determined by molecular replacement by using the program Molrep from the CCP4 program suite with two models of human NT-3 (PDB code 1NT3) and the partial C-terminal half of $p75^{NTR}$ from the NGF–$p75^{NTR}$ 2:1 asymmetric complex (PDB code 1SG1) as the initial search models. The phases obtained were improved by using RESOLVE[26], and the structure of the remaining part of $p75^{NTR}$ was independently traced by Coot into clear difference Fourier maps and refined with Refmac; no non-crystallographic symmetry restraints were used in the refinement. The software packages Refmac and Coot were used to complete the model and refine it to a final R_{work}/R_{free} value of 22.4%/28.8%. Statistics for data collection and refinement are provided in Supplementary Table 2. The quality of the final structure was evaluated with PROCHECK[27]. A Ramachandran plot showed that most of the residues were in the favourable region (80.4%) and that no residues were in the generously allowed and disallowed regions.

Analytical ultracentrifugation. Sedimentation velocity experiments were performed on a Beckman XL-I analytical ultracentrifuge at 20 °C. Protein samples were diluted with PBS to 400 μl at a concentration of about 0.3 mg ml^{-1}. Data were collected at 60,000 r.p.m. (262,000g) every 3 min at a wavelength of 280 nm. Interference sedimentation coefficient distributions, $c(M)$, were calculated from the sedimentation velocity data by using SEDFIT[28].

BIAcore analysis. Real-time binding and kinetic analyses by surface plasmon resonance were performed on a BIAcore 3000 instrument (Pharmacia Biosensor AB). The eluent contained PBS and 0.005% Tween 20. Human NT-3 was immobilized on a CM5 chip by using an amine coupling kit, and the remaining coupling sites were blocked with 1 M ethanolamine (pH 8.5). Binding was evaluated over a range of $p75^{NTR}$ (25–800 nM) or dg-$p75^{NTR}$ (50–1,200 nM) concentrations at 25 °C. Kinetic parameters were further determined with BIAevaluation 4.1 software.

26. Terwilliger, T. C. Maximum-likelihood density modification. *Acta Crystallogr. D Biol. Crystallogr.* **56,** 965–972 (2000).
27. Laskowski, R. A., MacArthur, M. W., Moss, D. S. & Thornton, J. M. PROCHECK: a program to check the stereochemical quality of protein structures. *J. Appl. Crystallogr.* **26,** 283–291 (1993).
28. Schuck, P. Size-distribution analysis of macromolecules by sedimentation velocity ultracentrifugation and Lamm equation modeling. *Biophys. J.* **78,** 61606–61619 (2000).